

Specific Features of the Microstructure and Properties of Multielement Nitride Coatings Based on TiZrNbAlYCr

A. D. Pogrebnjak^{a*}, V. M. Beresnev^b, O. V. Bondar^a, Ya. O. Kravchenko^a,
B. Zhollybekov^c, and A. I. Kupchishin^d

^a Sumy State University, 40007 Sumy, Ukraine

^b Karazin Kharkiv National University, 61022 Kharkiv, Ukraine

^c Berdakh Karakalpak State University, Nukus, 230112 Uzbekistan

^d Abai Kazakh National Pedagogical University, Almaty, 050010 Kazakhstan

*e-mail: alexp@i.ua

Received April 17, 2017

Abstract—Multicomponent nanostructured coatings based on (TiZrNbAlYCr)N with a hardness as high as 47 GPa were obtained by cathodic arc deposition. The effect of partial nitrogen pressure P_N (with constant bias potential $U_b = -200$ V applied to the substrate) on the phase-composition variation, the size of crystallites, and their relation to the microstructure and hardness was investigated. An increase in the nitrogen pressure resulted in the formation of two phases with characteristic BCC (the lattice period is 0.342 nm) and FCC lattices with averaged nanocrystallite sizes of 15 and 2 nm. At a high pressure of 0.5 Pa, crystallites in the FCC phase with a lattice period of 0.437 nm grew in size to ~ 7 nm. The hardness of deposited coatings with larger (3.5 nm) FCC-phase crystallites and smaller (7 nm) BCC-phase crystallites was enhanced considerably.

DOI: 10.1134/S1063785018020098

High-entropy alloys (HEAs) with at least five atoms of transition and refractory metals are now used extensively in both fundamental (synthesis of new coatings and examination of their properties and structure) and applied (fabrication of products with such coatings and their application in various fields ranging from biocompatible implants to space technology) research [1–6]. The synthesis of HEA nitrides and carbides provides an opportunity to improve such material parameters as their radiation hardness, wear resistance, corrosion resistance, etc. A large number of different multielement alloys (including ones with high entropies of mixing) have already been obtained and studied [7–10], but nitride coatings based on these alloys quite rarely exhibit the needed physical and mechanical properties. Therefore, the problem of synthesis of nitride coatings based on multielement alloys with fine hardness, wear-resistance, and corrosion-resistance parameters remains important. In the present study, a new composition of nitride coatings based on the TiZrNbAlYCr multielement alloy is proposed and the results of examination of their structure and properties are detailed.

Coatings were obtained by cathodic-arc deposition onto stainless-steel substrates at different partial nitrogen pressures (0.05, 0.27, and 0.5 Pa). A Bulat-6 setup was used in these experiments. Constant bias potential $U_b = -200$ V was applied to the substrate in the process

of deposition. Substrate temperature T_s was approximately 300°C, and the distance to the cathode was 200 mm. Multielement coatings were deposited in the direct (unfiltered) flow regime, with the arc current being 100 A and the focusing-coil current being 0.5 A. The deposition was performed using a composite cathode with the following composition: 25 at % Ti, 20 at % Zr, 20 at % Nb, 25 at % Cr, 7 at % Al, and 3 at % Y. An SPS 25-10 spark-plasma sintering setup was used to fabricate this cathode. The deposition time was 1 h, and the overall thickness was 7.0 μm . The structure-phase state of the deposited coatings was studied with an X'Pert PAN analytical diffractometer at a pitch of 0.05°, and the microhardness was measured with a DM-8 tester at a load of 50 g.

The profiles were decomposed into constituent fragments in PowderCell. A JEM-7001 TTLS scanning electron microscope (JEOL) with an EDS microprobe operating in the SEI and Compto modes was used for elemental analysis and to examine the cross sections of coatings.

The results of examination of the surface morphology of coatings obtained under different partial nitrogen pressures (0.05, 0.27, and 0.5 Pa) demonstrate that an increase in pressure results in a reduction in the average size of drop phases on the coating surface: their characteristic size varies from 1.1 μm at 0.05 Pa to 0.2 μm at 0.5 Pa. One of the reasons for this is the

emergence of cathode spots of the first type (together with cathode spots of the second type) [7] with a notably lower erosion factor. This speeds up the return of particles to the cathode as a result of collisions with gas atoms and molecules. However, the most significant reduction in the erosion factor is observed when high-melting gas–metal compounds (such as TiN) with elevated melting temperatures form on the cathode surface [11].

The results of elemental analysis are presented in Table 1 and Fig. 1. It can be seen that the coatings deposited under higher pressures are saturated with nitrogen atoms and have higher concentrations of light Al atoms.

The study of the phase composition (Fig. 2) showed that the spectra of coatings formed under the lowest pressure $P_N = 0.05$ Pa contain a system of diffraction lines of a solid solution of metal atoms with a characteristic BCC lattice with a period of 0.342 nm and an average crystallite size of 15 nm.

The decomposition of the diffraction curve into constituent profiles (Fig. 2a) revealed the formation of nanocrystalline structures with ordered regions ~ 2 nm in size. These structures in the coating manifest themselves as a wide halolike profile visible at large angles in the diffraction spectra.

The peak corresponding to the BCC-phase crystallites in the diffraction spectrum of the (TiZrNbAlYCr)N coating obtained at 0.27 Pa (see spectrum 2 in Figs. 1b, 2b) is close in position and width to the one discussed above. The halolike diffuse peak of the second component evolves into a more ordered peak shifted toward larger diffraction angles. The calculation based on reflection broadening yields a value of ~ 3.5 nm. In view of the emergence of another peak at 60° , the obtained spectrum corresponds to a nitride phase with a NaCl[111]-type lattice.

The concentration of nitrogen in the coating deposited under the highest pressure $P_N = 0.5$ Pa exceeds 21 at % (see Fig. 1 and Table 1). The diffraction spectrum of this coating contains two well-pronounced systems of diffraction peaks of the BCC phase with a characteristic period of 0.342 nm and the FCC phase (of the NaCl structure type) with a characteristic period of 0.437 nm (Fig. 2c). The average crystallite size was 7 nm.

The second system of peaks in all spectra presumably represents the forming second FCC phase. The observed shift toward smaller angles, which is denoted by an arrow in Fig. 2, and the broadening of diffraction reflections at lower P_N values may then be attributed to the formation of stacking faults associated with the displacement of lattice planes that are not stabilized by nitrogen. This effect is induced by the bombardment of coatings by high-energy metal particles under a low pressure and with a negative bias potential ($U_b = -200$ V) applied

Table 1. Elemental composition of (TiZrNbAlYCr)N coatings deposited under different partial pressures of nitrogen atmosphere

Element	0.05 Pa		0.27 Pa		0.5 Pa	
	wt %	at %	wt %	at %	wt %	at %
N	2.1	8.9	0.5	2.3	4.7	21.6
Al	2.00	4.55	2.1	5.14	3.7	7.3
Y	4.26	2.99	4.37	3.22	4.47	2.6
Zr	24.31	16.32	26.10	18.77	22.95	14.0
Nb	27.49	18.13	28.85	20.38	23.9	14.2
Ti	21.75	27.82	19.77	27.08	21.32	25.0
Cr	18.09	21.29	18.31	23.11	18.96	15.3
Total	100.0	100.0	100.0	100.0	100.0	100.0

to the substrate. Large differences in the sizes of HEA atoms result in deformation of the film both on the microlevel and on the macrolevel and stimulate the formation of stacking faults. The mean energy of

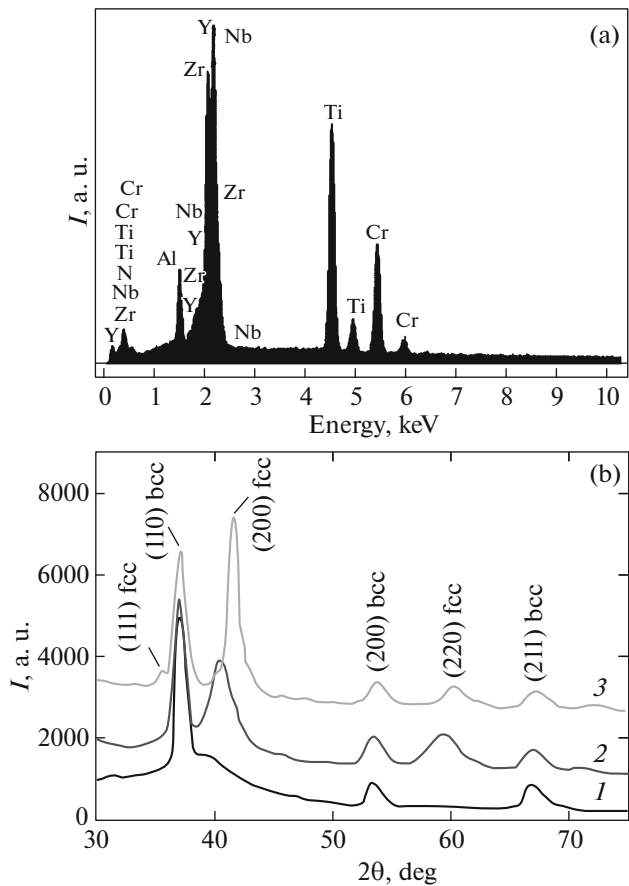


Fig. 1. (a) Energy-dispersive spectrum of the (TiZrNbAlYCr)N coating deposited at $P_N = 0.5$ Pa. (b) Regions of diffraction spectra of (TiZrNbAlYCr)N coatings obtained at $P_N = 0.05$ (1), 0.27 (2), and 0.5 Pa (3).

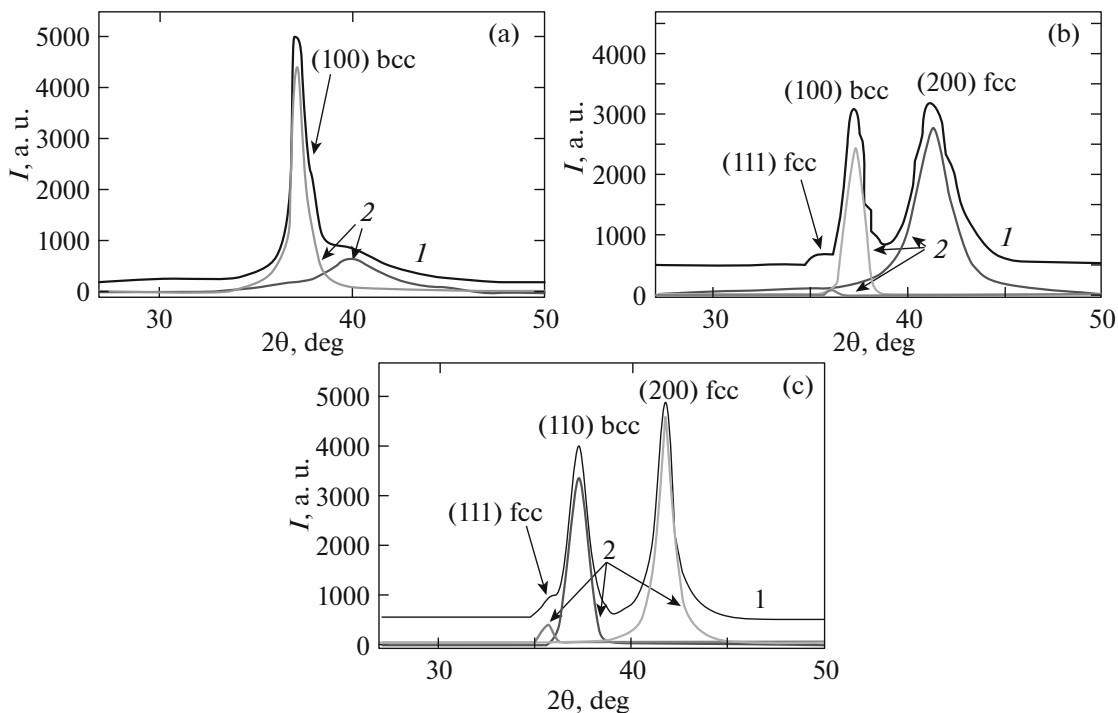


Fig. 2. X-ray of diffraction spectra of (TiZrNbAlYCr)N coatings obtained at $P_N =$ (a) 0.05, (b) 0.27, and (c) 0.5 Pa. The initial spectra (I) and the isolated profiles (2) are shown.

deposited particles, which is affected by losses in collisions within the interelectrode gap, decreases at higher working gas pressures in the chamber. In addition, coatings deposited under higher pressures are less deformed and more saturated with nitrogen atoms. Nitrogen atoms form chemical bonds with the metal framework and occupy octahedral interstitial sites characteristic of NaCl-type lattices. As a result, they inhibit the shear displacement of planes that causes the formation of stacking faults. The structural transformations that have been noted enhance the hardness of the coating deposited under the highest partial nitrogen pressure (0.5 Pa).

The results of microhardness measurements performed using a DM-8 tester with a load of 50 g show that the Vickers microhardness of (TiZrNbAlYCr)N coatings was $HV_{0.05} = 46.9$ GPa at $P = 0.5$ Pa. Therefore, these coatings may be characterized as superhard.

Thus, the variation of pressure in the deposition chamber from 0.05 to 0.5 Pa affects the morphology of (TiZrNbAlYCr)N coatings. Specifically, the drop component on the condensate surface is suppressed qualitatively and quantitatively at higher pressures. These changes in the structure-phase state translate into differences in mechanical properties. The measurement results suggest that the hardness increases to 46.9 GPa under a partial pressure of 0.5 Pa.

Acknowledgments. We wish to thank O.V. Sobol' for his help in interpreting the results of X-ray-diffraction analysis. This study was conducted as a part of budget programs nos. 0115U000682 "Research into the Materials-Science Foundations of Structure Engineering of Vacuum-Plasma Superhard Coatings with Required Functional Properties" and 0116U002621 "Physical Principles of Tailoring the Composition and Properties of Boride, Nitride, and Boron-Nitride Films Based on Transition Metals for Machine Engineering."

REFERENCES

1. A. D. Pogrebnjak, A. A. Bagdasaryan, I. V. Yakushchenko, and V. M. Beresnev, *Russ. Chem. Rev.* **83**, 1027 (2014).
2. D. B. Miracle and O. N. Senkov, *Acta Mater.* **122**, 448 (2017).
3. A. D. Pogrebnjak, I. V. Yakushchenko, O. B. Bondar, V. M. Beresnev, K. Oyoshi, O. M. Ivasichin, H. Amekura, Y. Takeda, M. Opielak, and C. Kozak, *J. Alloys Compd.* **679**, 155 (2016).
4. A. D. Pogrebnjak, I. V. Yakushchenko, A. A. Bagdasaryan, O. V. Bondar, R. Krause-Rehberg, G. Abadiaz, P. Chartier, K. Oyoshi, Y. Takeda, V. M. Beresnev, and O. V. Sobol, *Mater. Chem. Phys.* **147**, 1079 (2014).

5. V. Braic, A. Vladesku, M. Balaceanu, C. R. Luculescu, and M. Braic, *Surf. Coat. Technol.* **211**, 117 (2012).
6. I. V. Kireeva, I. V. Chumlyakov, Z. V. Pobedennaya, A. V. Vyrodova, A. V. Kuksgauzen, V. V. Poklonov, and D. A. Kuksgauzen, *Tech. Phys. Lett.* **43**, 615 (2017).
7. A. D. Pogrebnjak, *J. Nanomater.* **2013**, 780125 (2013).
8. Y. Zhang, T. T. Zuo, Z. Tang, M. C. Cao, K. A. Dahmen, P. K. Liaw, and Z. P. Lu, *Prog. Mater. Sci.* **61**, 1 (2014).
9. D. C. Tsai, Z. C. Chang, B. H. Kuo, M. H. Shiao, S. Y. Chang, and F. S. Shieu, *Appl. Surf. Sci.* **282**, 789 (2013).
10. M. H. Tsai, C. W. Wang, C. H. Lai, J. W. Yeh, and J. Y. Gan, *Appl. Phys. Lett.* **92**, 052129 (2008).
11. A. A. Andreev, L. P. Sablev, and S. N. Grigor'ev, *Vacuum-Arc Coatings* (Khark. Fiz. Tekh. Inst., Kharkov, 2010) [in Russian].

Translated by D. Safin